

## Overview of rare B-decays

---

**Jessica Prisciandaro**<sup>\*†</sup>

*Universidade de Santiago de Compostela (ES)*

*E-mail:* [jessica.prisciandaro@cern.ch](mailto:jessica.prisciandaro@cern.ch)

Being extremely suppressed in the Standard Model, rare decays of heavy-flavoured particles are a powerful probe of New Physics, and allow to reach energies beyond those accessible through direct searches. Several new results have been obtained by the LHC experiments. In particular,  $b \rightarrow sl^+l^-$  transitions give access to a large spectrum of observables, which provide complementary information on possible New Physics contributions. In this sector, tensions with Standard Model predictions have been observed.

*The 15th International Conference on Flavor Physics & CP Violation*

*5-9 June 2017*

*Prague, Czech Republic*

---

<sup>\*</sup>Speaker.

<sup>†</sup>On behalf of the LHCb collaboration.

## 1. Introduction

In the Standard Model (SM), flavour changing interactions are mediated by the charged weak bosons. Transitions among the different quark flavours are regulated by the Cabibbo-Kobayashi-Maskawa (CKM) quark mixing matrix, which is approximately diagonal [1]. Any direct transition among the *up* or *down* type quarks, namely flavour-changing-neutral-current (FCNC) transitions, are forbidden at tree level, making these processes rare in the SM. FCNCs provides a large variety of observables which are precisely predicted in the SM, i.e. branching fractions, angular observables, CP asymmetries, and which may be interested by important deviations from the SM in case of New Physics (NP), as predicted by several Beyond the Standard Model (BSM) theories.

Rare decays cover a large variety of physical processes, they can be divided according to their final state, or depending on the parent hadron involved in the decay process. In the former case, we can talk about purely leptonic decays, with only leptons in the final state (e.g.  $B_{(s)}^0 \rightarrow \mu^+ \mu^-$ ); semileptonic decays, where both hadrons and leptons are present in the final state (e.g.  $B_{(s)}^0 \rightarrow K^* \mu^+ \mu^-$ ); and radiative decays, where a radiated photon is also involved. In the latter case, we can split rare decays in B-meson, D-meson and strange (if *strange* quarks are involved) decays, or baryonic decays if the decaying particle is a baryon instead of a meson.

Rare decays theoretical description is particularly challenging because of the different scales involved, from the small QCD scale ( $\Lambda_{QCD} \approx 0.2$  GeV) to the large scale which would govern New Physics. To face this, FCNC transitions can be described by means of an effective field theory in which short and long distance contribution are separated, and which describe the transition as an Operator Product Expansion [2]. For  $b \rightarrow s$  transitions the effective Hamiltonian can be written has:

$$\mathcal{H}_{eff} = -\frac{4G_F}{\sqrt{2}} V_{tb} V_{ts}^* \frac{e^2}{16\pi^2} \sum_i [C_i(\mu) O_i(\mu) + C'_i(\mu) O'_i(\mu)] \quad (1.1)$$

where  $G_F$  is the Fermi constant and  $V_{ij}$  are CKM matrix elements. The Wilson coefficients,  $C_i$ , contain the perturbative, short distance effects, while the non perturbative QCD and long distance physics is encoded in the operators  $O_i$ . New physics effects can be described either by a modification of a Wilson coefficient or by the appearance of a new operator not present in the SM. The sensitivity to different operators and Wilson coefficients depends on the decay topology and on the  $q^2$  region of interest (as shown in Fig. 1 for  $b \rightarrow sl^+l^-$  processes), where  $q^2$  denotes the invariant mass squared of the lepton pair. Table 1 summarises the operators that contribute to radiative, purely leptonic and semileptonic decays.

In this document I present a selection of the rare decays sector results from the LHCb, CMS, ATLAS and Belle experiments.

## 2. Fully leptonic meson decays

The  $B^0 \rightarrow \mu^+ \mu^-$  and  $B_s^0 \rightarrow \mu^+ \mu^-$  decays, are very rare in the SM. They can occur only through loop diagrams and are helicity suppressed. Given their purely leptonic final state, and thanks to the very precise lattice QCD calculations, their branching fraction (BF) is very precisely

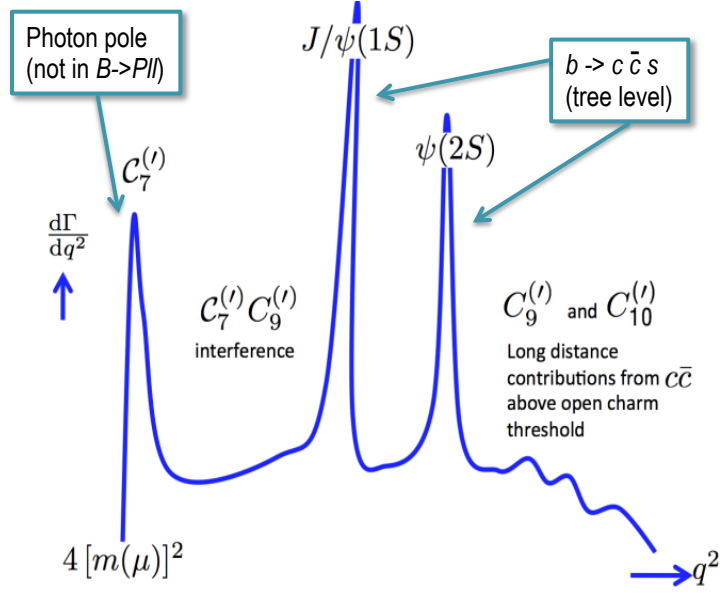


Figure 1: Differential branching fraction as a function of the dimuon invariant mass squared,  $q^2$ , for  $b \rightarrow sl^+l^-$  processes. Depending on the  $q^2$  region analysed, different Wilson coefficients can be probed.

Table 1: Operators that contribute to rare  $B$  decays.  $O_7$ ,  $O_9$  and  $O_{10}$  are the *electromagnetic penguin*, *vector semileptonic* and *axial-vector semileptonic* operators, respectively; while  $O_S$  and  $O_P$  are the *scalar* and *pseudoscalar* operators.

Operator	$B_{d,s} \rightarrow X\mu^+\mu^-$	$B_{d,s} \rightarrow \mu^+\mu^-$	$B_{d,s} \rightarrow X\gamma$
$O_7$	✓		✓
$O_9$	✓		
$O_{10}$	✓	✓	
$O_S$		✓	
$O_P$		✓	

predicted in the SM [3],

$$\begin{aligned} \mathcal{B}(B^0 \rightarrow \mu^+\mu^-) &= (1.06 \pm 0.09) \times 10^{-10}, \\ \mathcal{B}(B_s^0 \rightarrow \mu^+\mu^-) &= (3.66 \pm 0.23) \times 10^{-9}. \end{aligned} \quad (2.1)$$

Several BSM theories predict NP scalar or pseudoscalar operators, which might sizeable enhance their decay rate. In addition, the ratio of the branching fractions between the  $B$  and the  $B_s$  decay modes also provides powerful discrimination among BSM theories, since in case of NP with minimal flavour violation (MFV), it is not expected to diverge from the SM value.

Multiple searches for these decays have been carried on by the LHC experiments. The first observation of the  $B_s^0 \rightarrow \mu^+\mu^-$  decay at  $6.2\sigma$  significance, and evidence of the  $B^0 \rightarrow \mu^+\mu^-$  channel at  $3.0\sigma$  significance, have been published thanks to the combined analysis of the LHCb and CMS

collaboration [4]. The measured branching fractions,

$$\begin{aligned}\mathcal{B}(B^0 \rightarrow \mu^+ \mu^-) &= (3.0_{-1.4}^{+1.6}) \times 10^{-10}, \\ \mathcal{B}(B_s^0 \rightarrow \mu^+ \mu^-) &= (2.8_{-0.6}^{+0.7}) \times 10^{-9},\end{aligned}\quad (2.2)$$

are compatible with the SM predictions and put strong constraints on BSM theories. In addition, the measurements have been combined to determine the ratio of branching fractions, which deviates from the SM expectation by  $2.3\sigma$ . Figure 2 shows the fitted dimuon invariant mass spectrum and the variation of the test statistic  $-2\Delta\ln\mathcal{L}$  for  $\mathcal{B}(B_s^0 \rightarrow \mu^+ \mu^-)$ .

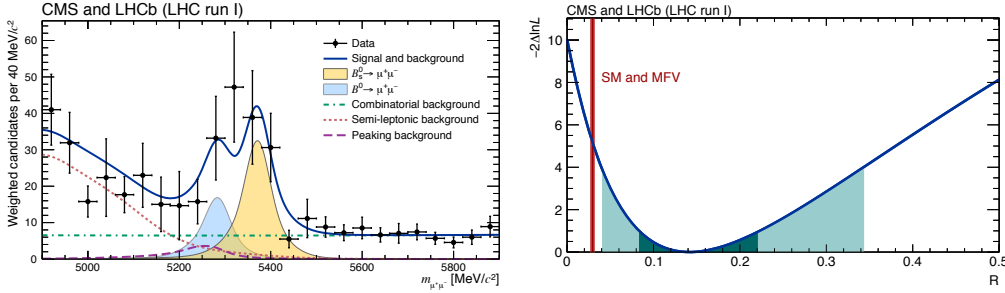


Figure 2: Weighted distribution of the dimuon invariant mass,  $m_{\mu^+\mu^-}$  with the fit superimposed (left), and variations of the test statistic  $-2\Delta\ln\mathcal{L}$  for  $\mathcal{B}(B_s^0 \rightarrow \mu^+ \mu^-)$  (right).

The ATLAS collaboration also found compatible results with CMS and LHCb, even if their measurement remains below the evidence level ( $2\sigma$ ) [5].

Recently, LHCb published an updated analysis of this decay [6], which led to the first observation by a single experiment of the  $B_s^0 \rightarrow \mu^+ \mu^-$  decay, at  $7.8\sigma$  significance, and to the best upper limit for the  $B^0$  mode. Besides the increased statistics, the measurement benefits from an improved analysis strategy. In particular, a better sensitivity is achieved thanks to a most performant multivariate selection, which makes use of a new signal isolation, and a better particle identification (PID) with a higher muon/pion discrimination power. The measured branching fractions are:

$$\begin{aligned}\mathcal{B}(B^0 \rightarrow \mu^+ \mu^-) &< 3.4 \times 10^{-10} \text{ at } 95\% \text{ CL}, \\ \mathcal{B}(B_s^0 \rightarrow \mu^+ \mu^-) &= (3.0 \pm 0.6 (\text{stat})_{-0.2}^{+0.3} (\text{syst})) \times 10^{-9}.\end{aligned}\quad (2.3)$$

The fitted mass distribution of the  $B_{(s)}^0 \rightarrow \mu^+ \mu^-$  candidates with  $\text{BDT} > 0.5$  and the likelihood contours in the  $\mathcal{B}(B_s^0 \rightarrow \mu^+ \mu^-)$  vs  $\mathcal{B}(B^0 \rightarrow \mu^+ \mu^-)$  plane are shown in Fig. 3.

The branching fraction measurement is not able, alone, to constrain all possible NP, given that it can not distinguish between scalar and pseudo-scalar contributions [7]. A complementary measurement to that of the branching fraction, is that of the decay width asymmetry,

$$A_{\Delta\Gamma} = \frac{\Gamma(B_s^H \rightarrow \mu^+ \mu^-) - \Gamma(B_s^L \rightarrow \mu^+ \mu^-)}{\Gamma(B_s^H \rightarrow \mu^+ \mu^-) + \Gamma(B_s^L \rightarrow \mu^+ \mu^-)}\quad (2.4)$$

In the SM only the heavy  $B_s$  mass eigenstate decays to two muons, which implies a decay width asymmetry  $A_{\Delta\Gamma} = 1$ , and a lifetime  $\tau_{\mu^+\mu^-} = 1.610 \pm 0.012$  ps. Together with the branching fraction measurement, LHCb published the first measurement of the  $B_s^0 \rightarrow \mu^+ \mu^-$  lifetime,  $\tau(B_s^0 \rightarrow$

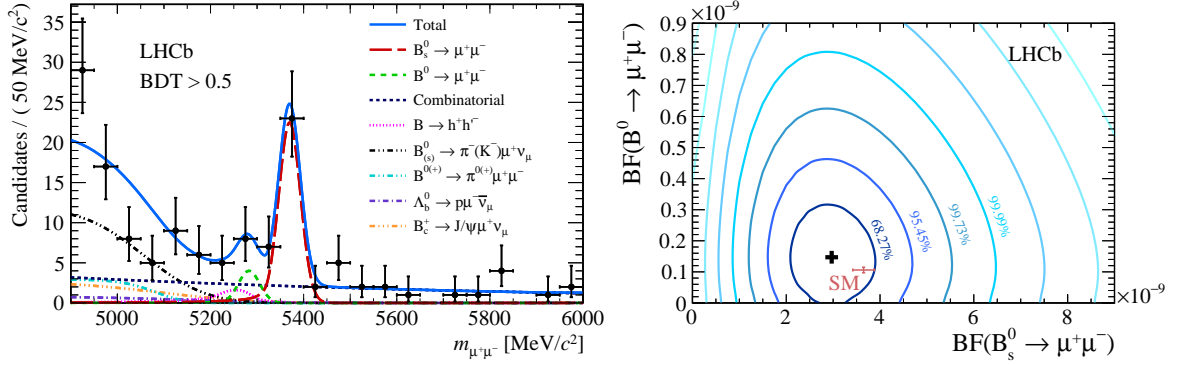


Figure 3: Mass distribution of the selected  $B_{(s)}^0 \rightarrow \mu^+\mu^-$  candidates with  $\text{BDT} > 0.5$  with the result of the fit is overlaid (left), and likelihood contours in the  $\mathcal{B}(B_{(s)}^0 \rightarrow \mu^+\mu^-)$  vs  $\mathcal{B}(B^0 \rightarrow \mu^+\mu^-)$  plane (right).

$\mu^+\mu^-) = 2.04 \pm 0.44(\text{stat}) \pm 0.05(\text{syst})$ . The measurement is compatible with  $A_{\Delta\Gamma} = 1(-1)$  at 1 (1.4)  $\sigma$  significance.

Another measurement of purely leptonic  $B$  decays performed by LHCb, is the search for the decay  $B_{(s)}^0 \rightarrow \tau^+\tau^-$  [8]. While the same considerations in terms of SM predictions and NP as for the  $B_{(s)}^0 \rightarrow \mu^+\mu^-$  decay mode are valid, the larger  $\tau$  mass, compared to that of the muon, makes this channel less helicity suppressed (branching fraction predicted to be  $\sim 100$  larger). In addition, MVF models which accommodate the recent results from the Lepton Flavour Universality (LFU) tests can lead to enhancement of its branching fraction up to a few percents. From the experimental side, the search for this channel is more demanding than that for the corresponding muonic decay, because of the presence of neutrinos in the final state. The  $\tau$  leptons are reconstructed in the  $\tau^- \rightarrow \pi^+\pi^-\pi^-\nu_\tau$  final state, and the  $B^0 \rightarrow D^+(K^-\pi^+\pi^-)D_s^-(K^+K^-\pi^-)$  mode is used as control channel. Since neither the  $B^0 \rightarrow \tau^+\tau^-$  nor  $B_s^0 \rightarrow \tau^+\tau^-$  has been experimentally observed, each limit on the branching fraction is set assuming no contribution from the other decay, resulting in

$$\begin{aligned} \mathcal{B}(B_s^0 \rightarrow \tau^+\tau^-) &< 6.8 \times 10^{-3} \text{ at } 95\% \text{ CL}, \\ \mathcal{B}(B^0 \rightarrow \tau^+\tau^-) &< 2.1 \times 10^{-3} \text{ at } 95\% \text{ CL}. \end{aligned} \quad (2.5)$$

These represent the best upper limits so far.

The last analysis of purely leptonic decays presented here, is that of the very rare strange decay  $K_s^0 \rightarrow \mu^+\mu^-$  [35], performed by the LHCb experiment.  $K_s^0 \rightarrow \mu^+\mu^-$  decays are expected to occur at a very low rate in the SM,  $\mathcal{B}(K_s^0 \rightarrow \mu^+\mu^-) = (5.0 \pm 1.5) \times 10^{-12}$  [36], but his branching fraction could be enhanced up to  $10^{-10}$  in case of NP. In order to measure the BF, the analysis performs a simultaneous fit in several BDT bins and two trigger categories. The  $K_s^0 \rightarrow \pi^+\pi^-$  decay mode, is used as normalization channel, as well as being the main background for this analysis. The best available upper limit is obtained,  $\mathcal{B}(K_s^0 \rightarrow \mu^+\mu^-) < 1 \times 10^{-9}$  at 95% CL. This analysis as well as the all strange physics program in LHCb is expected, in the near future, to largely benefit from the improved trigger available from the beginning of Run2, which will strongly increase the sensitivity to several rare and very rare strange mesons and baryon decays.

### 3. Semileptonic $b \rightarrow s(d)l^+l^-$ transitions

Semileptonic  $b \rightarrow s(d)l^+l^-$  transitions provide a rich spectrum of observables which are experimentally measurable with large enough precision to be sensitive to possible NP contributions. We can split  $b \rightarrow s(d)l^+l^-$  studies in three categories:

- Measurement of differential branching fractions in bins of  $q^2$ . The main limitation to those measurements comes from the large theoretical uncertainty due to hadronic form factors and non-factorisable hadronic effects.
- Angular analyses. They provide access to several observables which gives information complementary to that of the BF measurements. Moreover, it is possible to build observables that are free from form-factor uncertainties at leading order.
- Tests of lepton flavour universality. In the SM, branching fractions of semileptonic decays to final states containing  $e$ ,  $\mu$  and  $\tau$ , are expected to be the same except for lepton mass effects. Ratio of branching fractions are all the more a powerful test of the SM, since most of the theoretical uncertainties cancel in the ratio between the two channels involved.

#### 3.1 Differential branching fraction measurements

Several analyses of  $b \rightarrow sl^+l^-$  transitions have been performed by the LHCb collaboration. Figure 4 shows the differential branching fraction distributions as a function of  $q^2$  for  $B^+ \rightarrow K^+\mu^+\mu^-$ ,  $B^0 \rightarrow K^0\mu^+\mu^-$ ,  $B^+ \rightarrow K^{*+}\mu^+\mu^-$ ,  $B_s^0 \rightarrow \phi\mu^+\mu^-$ , and  $\Lambda_b \rightarrow \Lambda\mu^+\mu^-$  [9, 10, 11]. All the experimental measurements are compared with the theoretical predictions in the all  $q^2$  spectrum, excluding the  $cc$  resonance regions. Most of the experimental measurements tend to lie below the SM expectations across the full  $q^2$  range, especially in the region below  $\sim 6\text{GeV}^2/c^2$ , despite most of them are not significantly lower than the SM prediction. In addition to the above mentioned decays, the differential branching fraction of the  $B^0 \rightarrow K^*\mu^+\mu^-$  channel is measured by both the CMS [13] and LHCb [12] collaborations. The LHCb measurement includes for the first time the determination of the  $S$ -wave fraction of the  $K^-\pi^+$  system, which, previously, was treated as a systematic. The measurement of the  $S$ -wave fraction is compatible with theory predictions, and supports the previous estimates. As shown in Fig. 5, both measurements are in good agreement among each other and with the SM, despite the same pattern observed in the other  $b \rightarrow sl^+l^-$  transitions.

#### 3.2 Angular analysis of $B \rightarrow K^*\mu^+\mu^-$

A complementary approach to search for NP in  $b \rightarrow sl^+l^-$  transitions is the analysis of their angular distribution. One of the golden channels for angular analyses is  $B^0 \rightarrow K^*\mu^+\mu^-$ , which complex structure gives access to several observables sensitive to the  $C_7$ ,  $C_9$  and  $C_{10}$  Wilson coefficients and form factors. Angular analyses of this channel have been performed by the three LHC experiments, ATLAS [15], CMS [16] and LHCb [14], and by Belle [17]. The angular structure of the  $B^0 \rightarrow K^*\mu^+\mu^-$  decay can be fully described by three angles and  $q^2$ . Its CP-averaged differential branching fraction can be expressed as a function of the fraction of longitudinal polarisation of the  $K^{*0}$ ,  $F_L$ , the forward-backward asymmetry  $A_{FB}$ , and the CP-averaged terms  $S_i$ . Despite their

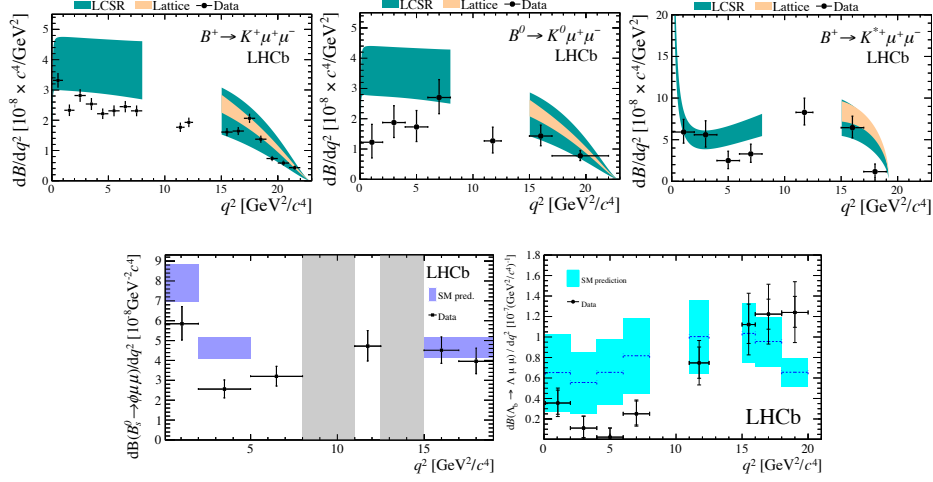


Figure 4: Differential branching fractions as a function of the dimuon invariant mass  $q^2$  for the  $B^+ \rightarrow K^+ \mu^+ \mu^-$ ,  $B^0 \rightarrow K^0 \mu^+ \mu^-$ ,  $B^+ \rightarrow K^{*+} \mu^+ \mu^-$ ,  $B_s^0 \rightarrow \phi \mu^+ \mu^-$ , and  $\Lambda_b \rightarrow \Lambda \mu^+ \mu^-$  decay channels. Theoretical predictions are superimposed.

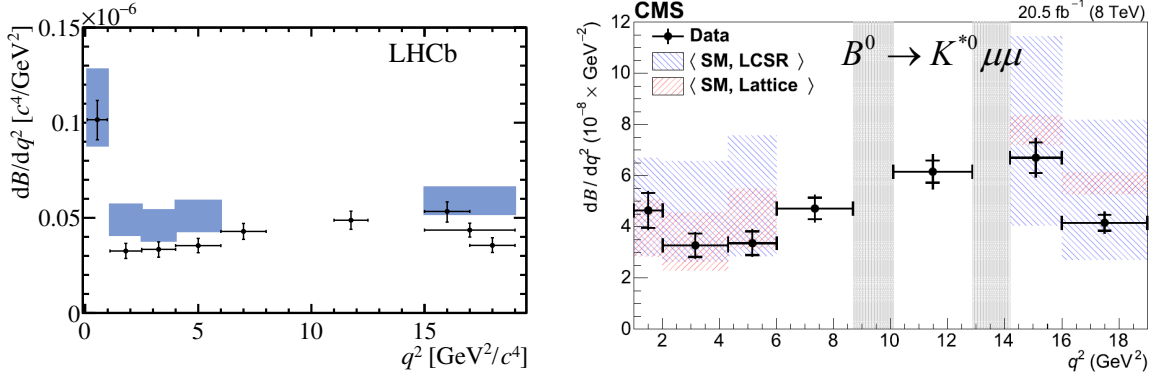


Figure 5: Differential branching fractions as a function of the dimuon invariant mass  $q^2$  for the  $B^0 \rightarrow K^{*0} \mu^+ \mu^-$  channel, measured by LHCb (right) and CMS (left). Theoretical predictions are superimposed.

sensitivity to possible NP, those variables are strongly affected by theoretical uncertainties. It is possible, however, to combine them in order to create a theoretically cleaner basis. In particular, the  $P'_i$  set of variables [18], such as  $P'_5 = S_5 / \sqrt{F_L(1 - F_L)}$ , are defined so that the dependence on form factors is reduced.

While most of the measured observables are in good agreement with the SM predictions, some discrepancies have been observed in the  $P'_5$  variable by LHCb, ATLAS and Belle. The deviation of the LHCb measurement from the SM is at the level of  $2.8 \sigma$  and  $3.0 \sigma$  for  $P'_5$ , in the bins  $4 < q^2 < 6 \text{ GeV}^2/c^4$  and  $6 < q^2 < 8 \text{ GeV}^2/c^4$ , respectively. Combining all the angular observables in the LHCb analysis, a global difference of  $3.4 \sigma$  from the SM expectation is observed.

In addition to the muonic channel, Belle measured also  $P'_4$  and  $P'_5$  for the electron channel. The difference  $Q'_i = P'_{i,\mu} - P'_{i,e}$ , expected to be 0 in the SM, can be used as lepton flavour universality test. While both measurements are compatible with the SM, a deviation of  $2.6\sigma$  is observed only for the muon channel, in good compatibility with the LHCb and ATLAS results. The same discrepancy is not observed in the electron channel, which point to the same direction of the LFU test results [19, 20]. Figure 6 compares the observed values for  $P'_5$  with the theoretical expectation in the muonic channel (left), and the measured  $P'_{5,\mu}$  and  $P'_{5,e}$  from Belle (right).

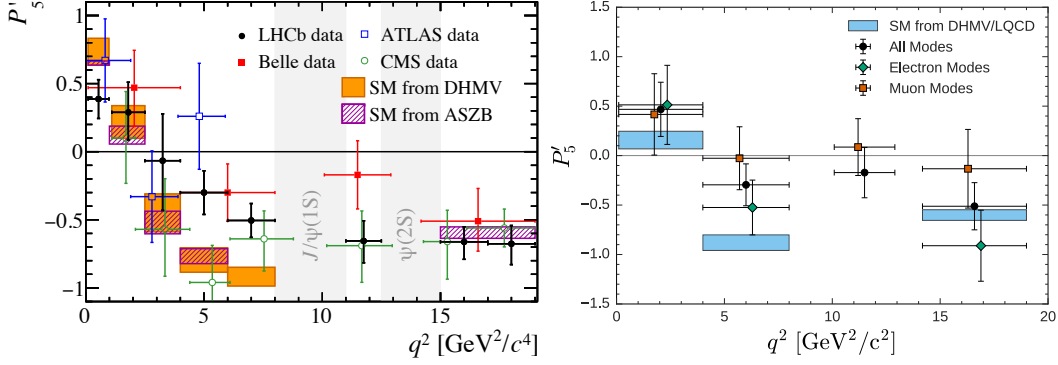


Figure 6: Comparison of  $P'_5$  as a function of  $q^2$  from LHCb, Belle, ATLAS and CMS, for the  $B^0 \rightarrow K^* \mu^+ \mu^-$  channel (left).  $P'_5$  distribution for  $B^0 \rightarrow K^* l^+ l^-$  decays from Belle (right).

### 3.3 Global fits and results interpretation

All the results showed so far, do not show a significant deviation from the SM if considered separately. However, it is possible to perform a combined analysis, which takes in account all the observables from  $b \rightarrow s(d)ll$ ,  $b \rightarrow ll$  and  $b \rightarrow h\gamma$  transitions, for a total of  $\sim 90$  variables, and all the experimental results. By those, so called, global fits, data-prediction deviations are minimised by varying the Wilson coefficient and allowing for NP contributions. As a result, a negative NP contribution with  $C_9 \sim -1$  seems to be preferred, with a significance of  $\sim 4 - 5\sigma$  [31, 32, 33, 34]. The interpretation of this result is not unambiguous. A first, more optimistic, scenario can explain those deviations as NP effect due to, for example, a  $Z'$  boson [21, 22, 23, 24, 25, 26] or leptoquarks [27, 28, 29]. On the other hand, those deviations could be the result of underestimated hadronic uncertainties, in particular contributions from the charm loop. To improve understanding, LHCb performed an analysis of the  $B \rightarrow K^+ \mu^+ \mu^-$  channel [30], including all the resonances and measuring the relative phases between the short-distance and the narrow-resonance amplitudes.

$$\frac{d\Gamma}{dq^2} = \frac{G_F^2 \alpha^2 |V_{tb} V_{ts}^*|^2}{128\pi^5} |k|\beta \left\{ \frac{2}{3} |k|^2 \beta^2 |C_{10} f_+(q^2)|^2 + \frac{4m_\mu^2 (m_B^2 - m_K^2)^2}{q^2 m_B^2} |C_{10} f_0(q^2)|^2 + |k|^2 \left[ 1 - \frac{1}{3} \beta^2 \right] \left| C_9 f_+(q^2) + 2C_7 \frac{m_b + m_s}{m_B + m_K} f_T(q^2) \right|^2 \right\}, \quad (3.1)$$

where  $m_B$ ,  $m_K$ ,  $m_b$ ,  $m_s$  and  $m_\mu$  are the masses of the mesons, quarks and leptons involved; the constants  $G_F$ ,  $V_{tq}$ , and  $\alpha$ , and are the Fermi constant, the relevant CKM matrix elements and the

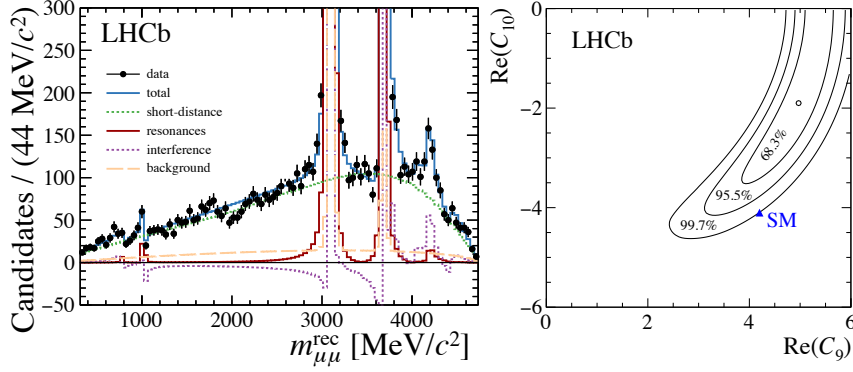


Figure 7: Fit to the dimuon mass distribution of the  $B^+ \rightarrow K^+ \mu^+ \mu^-$  events (left). Two-dimensional likelihood profile for the Wilson coefficients  $C_9$  and  $C_{10}$  (right).

QED fine structure constant;  $|k|$  denote the kaon momentum in the  $B^+$  meson rest frame;  $f_{0,+T}$  represents the scalar, vector and tensor  $B \rightarrow K$  form factors; and  $\beta^2 = 1 - 4m_\mu^2/q^2$ . Finally,  $C_i$  are the Wilson coefficients involved in the decay. This analysis takes in account in the Wilson coefficient the long-distance contribution, allowing all the magnitudes and relative phases between the resonances to vary in the fit to the dimuon mass spectrum (see Fig. 7 (left)). The interference between the resonant and non-resonant contribution is found to be small, and not able to explain the tension observed in  $P_5'$ . From the  $C_9$  and  $C_{10}$  two-dimensional likelihood profile, Fig. 7 (right), the fit prefers  $|C_9| > |C_9^{SM}|$  and  $|C_{10}| < |C_{10}^{SM}|$  if both free in the fit, and  $|C_9| < |C_9^{SM}|$  if  $C_{10}$  is constrained to the SM value. This is in agreement with the global fits results. The branching fraction of the short-distance component is found to be,

$$\mathcal{B}(B^+ \rightarrow K^+ \mu^+ \mu^-) = (4.37 \pm 0.15(\text{stat}) \pm 0.23(\text{syst})) \times 10^{-7} \quad (3.2)$$

in good agreement with the previous result from the exclusive analysis.

#### 4. Conclusions

Rare decays constitute powerful probes to test the SM and validate BSM theories, given the precise SM predictions, and the large expected contributions from NP. Many interesting results, only few of them covered here, have been published by various experiments, like LHCb, Belle, CMS and ATLAS. All the results, so far, are compatible with the SM predictions. Recently a pattern has emerged in global fits that might hint to NP. A lot of work is still required to clarify the tensions with the SM. New channels and observables have to be identified, and larger statistics will be needed in order to increase the sensitivity and clarify the still open questions.

#### References

- [1] S. L. Glashow, J. Iliopoulos and L. Maiani, “Weak Interactions with Lepton-Hadron Symmetry,” Phys. Rev. D **2** (1970) 1285. doi:10.1103/PhysRevD.2.1285

- [2] K. G. Wilson and W. Zimmermann, “Operator product expansions and composite field operators in the general framework of quantum field theory,” *Commun. Math. Phys.* **24**, 87 (1972).  
doi:10.1007/BF01878448
- [3] C. Bobeth, M. Gorbahn, T. Hermann, M. Misiak, E. Stamou and M. Steinhauser, “ $B_{s,d} \rightarrow l^+ l^-$  in the Standard Model with Reduced Theoretical Uncertainty,” *Phys. Rev. Lett.* **112**, 101801 (2014)  
doi:10.1103/PhysRevLett.112.101801 [arXiv:1311.0903 [hep-ph]].
- [4] V. Khachatryan *et al.* [CMS and LHCb Collaborations], “Observation of the rare  $B_s^0 \rightarrow \mu^+ \mu^-$  decay from the combined analysis of CMS and LHCb data,” *Nature* **522**, 68 (2015)  
doi:10.1038/nature14474 [arXiv:1411.4413 [hep-ex]].
- [5] M. Aaboud *et al.* [ATLAS Collaboration], “Study of the rare decays of  $B_s^0$  and  $B^0$  into muon pairs from data collected during the LHC Run 1 with the ATLAS detector,” *Eur. Phys. J. C* **76**, no. 9, 513 (2016) doi:10.1140/epjc/s10052-016-4338-8 [arXiv:1604.04263 [hep-ex]].
- [6] R. Aaij *et al.* [LHCb Collaboration], “Measurement of the  $B_s^0 \rightarrow \mu^+ \mu^-$  branching fraction and effective lifetime and search for  $B^0 \rightarrow \mu^+ \mu^-$  decays,” *Phys. Rev. Lett.* **118**, no. 19, 191801 (2017)  
doi:10.1103/PhysRevLett.118.191801 [arXiv:1703.05747 [hep-ex]].
- [7] K. De Bruyn, R. Fleischer, R. Kneijens, P. Koppenburg, M. Merk, A. Pellegrino and N. Tuning, “Probing New Physics via the  $B_s^0 \rightarrow \mu^+ \mu^-$  Effective Lifetime,” *Phys. Rev. Lett.* **109**, 041801 (2012)  
doi:10.1103/PhysRevLett.109.041801 [arXiv:1204.1737 [hep-ph]].
- [8] R. Aaij *et al.* [LHCb Collaboration], “Search for the decays  $B_s^0 \rightarrow \tau^+ \tau^-$  and  $B^0 \rightarrow \tau^+ \tau^-$ ,” *Phys. Rev. Lett.* **118**, no. 25, 251802 (2017) doi:10.1103/PhysRevLett.118.251802 [arXiv:1703.02508 [hep-ex]].
- [9] R. Aaij *et al.* [LHCb Collaboration], “Differential branching fractions and isospin asymmetries of  $B \rightarrow K^{(*)} \mu^+ \mu^-$  decays,” *JHEP* **1406**, 133 (2014) doi:10.1007/JHEP06(2014)133 [arXiv:1403.8044 [hep-ex]].
- [10] R. Aaij *et al.* [LHCb Collaboration], “Differential branching fraction and angular analysis of  $\Lambda_b^0 \rightarrow \Lambda \mu^+ \mu^-$  decays,” *JHEP* **1506**, 115 (2015) doi:10.1007/JHEP06(2015)115 [arXiv:1503.07138 [hep-ex]].
- [11] R. Aaij *et al.* [LHCb Collaboration], “Angular analysis and differential branching fraction of the decay  $B_s^0 \rightarrow \phi \mu^+ \mu^-$ ,” *JHEP* **1509**, 179 (2015) doi:10.1007/JHEP09(2015)179 [arXiv:1506.08777 [hep-ex]].
- [12] R. Aaij *et al.* [LHCb Collaboration], “Measurements of the S-wave fraction in  $B^0 \rightarrow K^+ \pi^- \mu^+ \mu^-$  decays and the  $B^0 \rightarrow K^*(892)^0 \mu^+ \mu^-$  differential branching fraction,” *JHEP* **1611**, 047 (2016)  
doi:10.1007/JHEP11(2016)047, 10.1007/JHEP04(2017)142, 10.1007/JHEP11(2016)047, 10.1007/JHEP04(2017)142 [arXiv:1606.04731 [hep-ex]].
- [13] V. Khachatryan *et al.* [CMS Collaboration], “Angular analysis of the decay  $B^0 \rightarrow K^{*0} \mu^+ \mu^-$  from pp collisions at  $\sqrt{s} = 8$  TeV,” *Phys. Lett. B* **753**, 424 (2016) doi:10.1016/j.physletb.2015.12.020 [arXiv:1507.08126 [hep-ex]].
- [14] R. Aaij *et al.* [LHCb Collaboration], “Angular analysis of the  $B^0 \rightarrow K^{*0} \mu^+ \mu^-$  decay using  $3 \text{ fb}^{-1}$  of integrated luminosity,” *JHEP* **1602**, 104 (2016) doi:10.1007/JHEP02(2016)104 [arXiv:1512.04442 [hep-ex]].
- [15] The ATLAS collaboration [ATLAS Collaboration], “Angular analysis of  $B_d^0 \rightarrow K^* \mu^+ \mu^-$  decays in pp collisions at  $\sqrt{s} = 8$  TeV with the ATLAS detector,” ATLAS-CONF-2017-023.
- [16] CMS Collaboration [CMS Collaboration], “Measurement of the  $P_1$  and  $P_5'$  angular parameters of the decay  $B^0 \rightarrow K^{*0} \mu^+ \mu^-$  in proton-proton collisions at  $\sqrt{s} = 8$  TeV,” CMS-PAS-BPH-15-008.

- [17] S. Wehle *et al.* [Belle Collaboration], “Lepton-Flavor-Dependent Angular Analysis of  $B \rightarrow K^* \ell^+ \ell^-$ ,” Phys. Rev. Lett. **118**, no. 11, 111801 (2017) doi:10.1103/PhysRevLett.118.111801 [arXiv:1612.05014 [hep-ex]].
- [18] S. Descotes-Genon, T. Hurth, J. Matias and J. Virto, “Optimizing the basis of  $B \rightarrow K^* \ell \ell$  observables in the full kinematic range,” JHEP **1305**, 137 (2013) doi:10.1007/JHEP05(2013)137 [arXiv:1303.5794 [hep-ph]].
- [19] R. Aaij *et al.* [LHCb Collaboration], “Test of lepton universality using  $B^+ \rightarrow K^+ \ell^+ \ell^-$  decays,” Phys. Rev. Lett. **113**, 151601 (2014) doi:10.1103/PhysRevLett.113.151601 [arXiv:1406.6482 [hep-ex]].
- [20] R. Aaij *et al.* [LHCb Collaboration], “Test of lepton universality with  $B^0 \rightarrow K^{*0} \ell^+ \ell^-$  decays,” JHEP **1708**, 055 (2017) doi:10.1007/JHEP08(2017)055 [arXiv:1705.05802 [hep-ex]].
- [21] R. Gauld, F. Goertz and U. Haisch, “An explicit  $Z'$ -boson explanation of the  $B \rightarrow K^* \mu^+ \mu^-$  anomaly,” JHEP **1401**, 069 (2014) doi:10.1007/JHEP01(2014)069 [arXiv:1310.1082 [hep-ph]].
- [22] S. Descotes-Genon, J. Matias and J. Virto, “Understanding the  $B \rightarrow K^* \mu^+ \mu^-$  Anomaly,” Phys. Rev. D **88**, 074002 (2013) doi:10.1103/PhysRevD.88.074002 [arXiv:1307.5683 [hep-ph]].
- [23] A. J. Buras, F. De Fazio, J. Girrbach and M. V. Carlucci, “The Anatomy of Quark Flavour Observables in 331 Models in the Flavour Precision Era,” JHEP **1302**, 023 (2013) doi:10.1007/JHEP02(2013)023 [arXiv:1211.1237 [hep-ph]].
- [24] W. Altmannshofer and D. M. Straub, “New Physics in  $B \rightarrow K^* \mu \mu$ ?,” Eur. Phys. J. C **73**, 2646 (2013) doi:10.1140/epjc/s10052-013-2646-9 [arXiv:1308.1501 [hep-ph]].
- [25] W. Altmannshofer, S. Gori, M. Pospelov and I. Yavin, “Quark flavor transitions in  $L_\mu - L_\tau$  models,” Phys. Rev. D **89**, 095033 (2014) doi:10.1103/PhysRevD.89.095033 [arXiv:1403.1269 [hep-ph]].
- [26] W. Altmannshofer, S. Gori, S. Profumo and F. S. Queiroz, “Explaining dark matter and B decay anomalies with an  $L_\mu - L_\tau$  model,” JHEP **1612**, 106 (2016) doi:10.1007/JHEP12(2016)106 [arXiv:1609.04026 [hep-ph]].
- [27] B. Gripaios, M. Nardecchia and S. A. Renner, “Composite leptoquarks and anomalies in  $B$ -meson decays,” JHEP **1505**, 006 (2015) doi:10.1007/JHEP05(2015)006 [arXiv:1412.1791 [hep-ph]].
- [28] D. Bećirević, S. Fajfer, N. Košnik and O. Sumensari, “Leptoquark model to explain the  $B$ -physics anomalies,  $R_K$  and  $R_D$ ,” Phys. Rev. D **94**, no. 11, 115021 (2016) doi:10.1103/PhysRevD.94.115021 [arXiv:1608.08501 [hep-ph]].
- [29] A. Crivellin, D. Müller and T. Ota, “Simultaneous Explanation of  $R(D^{(*)})$  and  $b \rightarrow s \mu^+ \mu^-$ : The Last Scalar Leptoquarks Standing,” arXiv:1703.09226 [hep-ph].
- [30] R. Aaij *et al.* [LHCb Collaboration], “Measurement of the phase difference between short- and long-distance amplitudes in the  $B^+ \rightarrow K^+ \mu^+ \mu^-$  decay,” Eur. Phys. J. C **77**, no. 3, 161 (2017) doi:10.1140/epjc/s10052-017-4703-2 [arXiv:1612.06764 [hep-ex]].
- [31] W. Altmannshofer, C. Niehoff, P. Stangl and D. M. Straub, “Status of the  $B \rightarrow K^* \mu^+ \mu^-$  anomaly after Moriond 2017,” Eur. Phys. J. C **77**, no. 6, 377 (2017) doi:10.1140/epjc/s10052-017-4952-0 [arXiv:1703.09189 [hep-ph]].
- [32] A. Paul and D. M. Straub, “Constraints on new physics from radiative  $B$  decays,” JHEP **1704**, 027 (2017) doi:10.1007/JHEP04(2017)027 [arXiv:1608.02556 [hep-ph]].
- [33] S. Descotes-Genon, L. Hofer, J. Matias and J. Virto, “Global analysis of  $b \rightarrow s \ell \ell$  anomalies,” JHEP **1606**, 092 (2016) doi:10.1007/JHEP06(2016)092 [arXiv:1510.04239 [hep-ph]].

- [34] T. Hurth, F. Mahmoudi, D. Martinez Santos and S. Neshatpour, “On lepton non-universality in exclusive  $b \rightarrow s\ell\ell$  decays,” arXiv:1705.06274 [hep-ph].
- [35] R. Aaij *et al.* [LHCb Collaboration], “Improved limit on the branching fraction of the rare decay  $K_s^0 \rightarrow \mu^+\mu^-$ ,” arXiv:1706.00758 [hep-ex].
- [36] G. Isidori and R. Unterdorfer, “On the short distance constraints from  $K(L,S) \rightarrow \mu^+\mu^-$ ,” JHEP **0401**, 009 (2004) doi:10.1088/1126-6708/2004/01/009 [hep-ph/0311084].